ELECTRON CLOUD SIMULATIONS FOR DAΦNE*

T. Demma, R. Cimino, S. Guiducci, C. Vaccarezza, and M. Zobov
INFN-LNF, Frascati, Italy

Abstract

After the first experimental observations compatible with the presence of the electron cloud effect in the DAΦNE positron ring, a systematic study has been performed regarding the electron cloud build-up. To assess the effects of the electron cloud, simulations of the cloud build up were carried out using ECLOUD [1]. The obtained numerical results are compared with experimental observations.

INTRODUCTION

After the 2003 shutdown for the FINUDA detector installation, and some optics and hardware modifications, the appearance of a strong horizontal instability for the positron beam at a current $I \approx 500mA$, triggered the study of the e-cloud effect in the DAΦNE collider. Experimental observation that seems to provide an evidence that the electron cloud effects are present in the DAΦNE positron ring can be summarized as follow: a larger positive tune shift is induced by the positron beam current [2]; the horizontal instability rise time cannot be explained only by the beam interaction with parasitic HOM or resistive walls and increase with bunch current [3]; the anomalous vacuum pressure rise with beam current in positron ring [4], bunch-by-bunch tune shifts measured along the DAΦNE bunch train present the characteristic shape of the electron cloud build-up [5]. There are also indications that wigglers play an important role in the instability, since the main changes after the 2003 shutdown were the modification of the wiggler poles, and lattice variation which gave rise to an increase of the horizontal beta functions in wigglers [6]. To better understand the electron cloud effects and possibly to find a remedy, a detailed simulation study is undergoing. In this communication we present recent simulation results relative to the build up of the electron cloud in the DAΦNE wiggler and in straight sections in presence of a solenoid magnetic field. When possible simulation results are compared to experimental observation. Conlusions follow in the last section.

BUILD UP IN THE WIGGLER

The wiggler magnetic field characterization was performed measuring the vertical magnetic field component B_y, over a rectangular point matrix on the x-z plane [7].

Table 1: DAΦNE beam and pipe parameters used as input for ECLOUD simulations.

parameter	unit	value
bunch population N_b	10^{10}	2.1
number of bunches N	–	100
missing bunches N_{gap}	–	20
bunch spacing L_{sep}	m	0.8
bunch length σ_z	mm	18
bunch horiz. size σ_x	mm	1.4
bunch vert. size σ_y	mm	0.05
wiggler chamber horiz. aperture $2h_x$	mm	120
wiggler chamber vert. aperture $2h_y$	mm	20
straight sections radius	mm	44
primary photo-emission yield $d\lambda/ds$	–	0.0088
photon reflectivity	–	50%
maximum SEY δ_{max}	–	1.9
energy for max. SEY E_{max}	eV	250

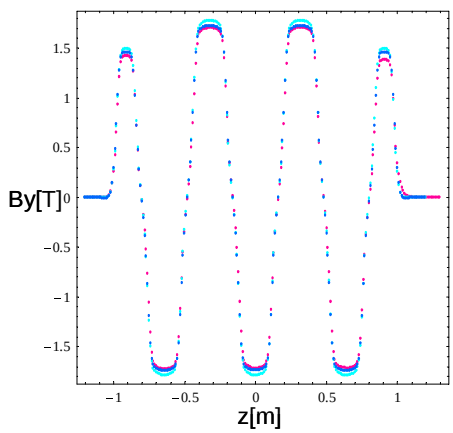

Figure 1: Vertical component of the magnetic field along the longitudinal axis for the old (blue), current (red), and recently proposed (cyan) wiggler.

Starting form these values a spline fit was performed, and the obtained coefficients were used for the field reconstruction as showed in [4]. This method has been applied to build three models of the wiggler field, the first corresponding to the wiggler before the pole modification in 2003, the second corresponding to the field after the pole modification (currently installed at DAΦNE), and the third corresponding to a further modification of the wiggler recently proposed to improve field quality and reduce nonlinearities [8]. In Figure 1 the field reconstruction results are reported

* This work is partly supported by the Commission of the European Communities under the 6^{th} Framework Programme "Structuring the European Research Area", contract number RIDS-011899.

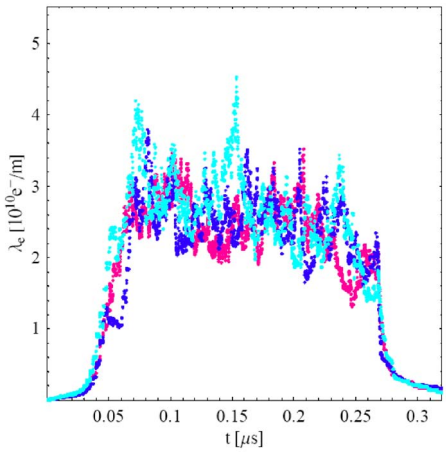

Figure 2: Electron cloud build up along a DAΦNE bunch train for the old (blue), current (red), and recently proposed (cyan) wiggler.

for the three different models. Using these models of the DAΦNE wiggler field, the electron build-up was simulated. The input parameters for ECLOUD are collected in Table 1. The reflectivity and photo-emission yield values have been obtained by measurements performed on Al samples with the same finishing of the actual vacuum chamber [9]. The secondary emission yield (SEY) curve model used is the one described in [10] scaled to an elastic reflection probability at zero electron energy of 0.5 [11], and with a maximum value $\delta_{max} = 1.9$ as were found for technical Al surfaces after electron conditioning [12]. It has to be noted that the presence of the slots has been taken into account considering only the photon flux that is not intercepted by the antechamber ($\approx 5\%$). With this prescription part of the electrons are emitted at the position of the antechamber slots. However, since in a dipole magnetic field these electrons contribute little to the multipacting and the electron build up, this approximation does not introduce any noticeable error. In Figure 2 the electron cloud linear density evolution is reported for the three wiggler magnetic field models discussed above, showing a negligible dependence of the build up on the magnetic field model. A very preliminary comparison with observations has been performed considering the horizontal instability growth rate dependence on the bunch spacing obtained by grow-damp measurement [3]. In particular, the values of bunch spacing L_{sep} and bunch population N_b corresponding to a growth rate $1/\tau \approx 8ms^{-1}$ has been extrapolated from recorded data, shown in Figure 3, and used as input for the simulation code. The resulting build up evolutions are shown in figure 4. The electron line densities corresponding to spacing by L_{sep} , $2L_{sep}$, and $3L_{sep}$ are comparable at the end of the train, while density corresponding to $4L_{sep}$ is about 3 times lower. This behaviour is in qualitative agreement with observations [3]. However, a deeper understanding of the instability mechanism would be gained comparing simulated single and multi-bunch growth rate with experimental data. Work in this direction is in progress.

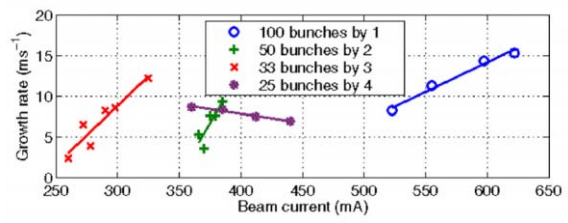

Figure 3: Horizontal growth rate for different bunch spacing and beam current recorded at DAΦNE on July 22, 2004 [3] (courtesy A.Drago).

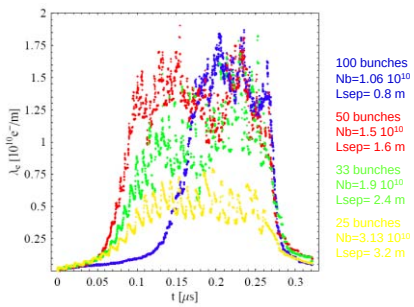

Figure 4: Electron cloud evolution along a bunch train for the measured values of L_{sep} and N_b corresponding to $1/\tau \approx 8ms^{-1}$.

BUILD UP IN SOLENOIDAL FIELD

At the startup after the recent shutdown for the setup of the crab waist collision scheme [13] the instability threshold dropped to $I \approx 270mA$ for the positron current, with the vertical feedback switched off. In the attempt to find a remedy solenoids were installed in the field free regions of DAΦNE, leading to an increase of the threshold to $I \approx 400mA$. Simulations followed to better understand this mechanism. Here we focus our attention on the electrons accumulated through the secondary emission from the beam pipe in the straight sections. In the simulation, we generate a large number of electrons only at the first bunch passage and let electron cloud develops by the secondary emission process. The electron cloud density build up along the train is shown in Figure 5, for different values of the solenoidal field B_z. Without solenoids (black curve in Figure 5) the average density grows along the train and saturates due to the balance between the space charge and secondary yield. For $Bs > 20G$ electron density decrease very quickly after the passage of the first bunch. A resonance is expected when the time between two consecutive collisions of the electrons in the cloud with the beam pipe surface, that is about half of the electrons cyclotron period T_c, is equal to the time interval between two bunch passage. For the DAΦNE parameters, this condition reads to

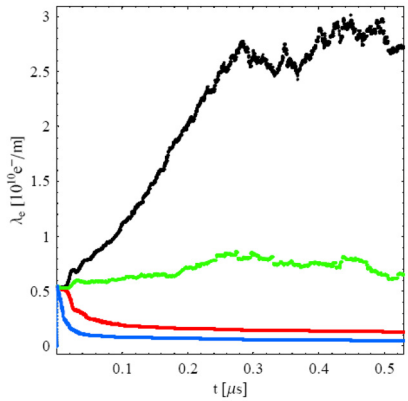

Figure 5: Density of electron cloud as a function of time for different solenoid settings: $B_z = 0G$ (black), $B_z = 20G$ (green), $B_z = 40G$ (red), $B_z = 60G$ (blue).

the following resonance condition for the magnetic field:

$$B_z^c = \frac{\pi m_e c^2}{eL_{sep}} \approx 66G. \quad (1)$$

However there is a threshold value of bunch population, related to the energy gain of the electrons in the cloud during the passage of a bunch and independent of the bunch spacing [14], above which the resonance takes place. As shown in Figure 6, simulations for DAΦNE exhibit a threshold $N_b^c \approx 5{\cdot}10^{10}$ for both single and double bunch spacing that is above the currently operated current. The effectiveness

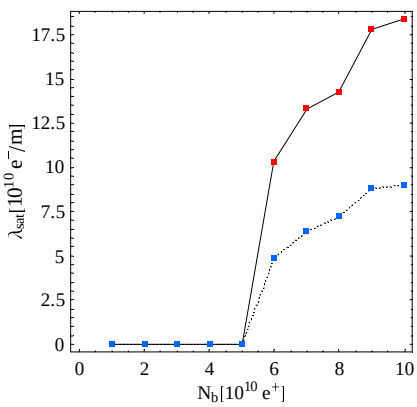

Figure 6: Saturated density as a function of the bunch population. Red dots represent the case of L_{sep} spacing and 66G field. Blue dots represent $2L_{sep}$ spacing and 33G field.

of solenoids in reducing the electron cloud density has also been checked by monitoring the vacuum behaviour for the positron beam. The vacuum pressure read-out is reported in Figure 7 for the solenoid ON-OFF cases as recorded by a vacuum gauge located in a region of the positron ring where solenois are installed. The pressure reduction in the region with solenoids is clear.

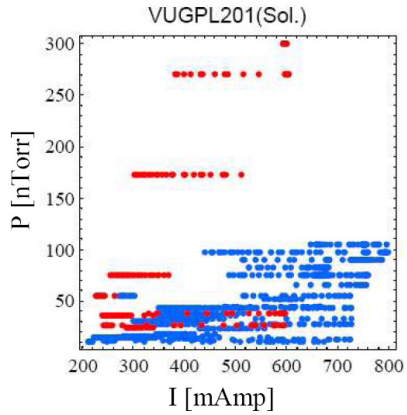

Figure 7: vacuum pressure read-out vs. total current as recorded in a straight section of the positron ring where a 40 G solenoidal field was turned on (blue dots) and off (red dots).

CONCLUSIONS

Simulations for the DAΦNE wiggler show a negligible dependence of the build up on the magnetic field model, and a build-up variation with bunch filling pattern that is compatible with experimental observations. Simulations for the build up in solenoidal field show that a small field is effective in reducing the electron cloud density in straight section, and that the threshold for the cyclotron resonance is above the bunch population currently available in DAΦNE. Also in this case there is a qualitative agreement with observations.

REFERENCES

[1] http://wwwslap.cern.ch/electron-cloud/Programs/ECLOUD /ecloud.html.

[2] C. Vaccarezza, et al, ECLOUD04, Napa Valley proc.

[3] A.Drago et al., Proceedings of PAC05, p.1841.

[4] C.Vaccerezza et al., Proceedings of PAC05, p.779.

[5] A.Drago, proc. of the 40th ICFA Beam Dynamics Workshop on High Luminosity e+e- Factories.

[6] A.Drago et al., DAΦNE Tech. Notes, G-67.

[7] M. Preger, DAΦNE Tech. Notes, L-34.

[8] S.Bettoni et al., Proceedings of PAC07, p. 1463.

[9] N.Mahne et al., Proceedings of PAC05, p.817.

[10] R. Cimino et al., PRL93, 014801, 2004;

[11] D.Schulte et al., PAC-2005-FPAP014, 2005.

[12] F. Le Pimpec et al., SLAC-PUB-10894 (2004).

[13] C.Milardi et al.,WEPP036, these proceedings.

[14] Y.Cai et al., Phys. Rev. ST-AB 7, 024402 (2004).